

A Numerical Method Predicting the Paper Velocity at the Roller Transfer Unit in an Electrophotographic System

*Satoshi Okano, Osamu Takehira and Yuko Hayama
Environmental Technology Research and Development Center
Ricoh Co. Ltd., Yokohama, Japan*

Abstract

A numerical method that predicts the paper velocity at the roller transfer unit in an electrophotographic system is presented including the roller slip characteristics and the tension in the paper. The roller slip characteristics are derived from the measurement of the relative velocity between the roller and a paper under an external force. The paper feeding simulation is used to calculate the tension in the paper among the registration rollers, the roller transfer unit and the fuser rollers. The paper velocity at the roller transfer unit is predicted solving the equilibrium equation between the tractions given by the transfer roller and the photoreceptor drum and the tensions in the paper. The predicted velocities agree well with those from experiments, which is based on the time interval sensing of the pattern of lines printed on papers.

Introduction

The roller transfer unit shown in Figure 1 is adopted in the middle class and the low one in electrophotographic machines, and is mainly composed of the photoreceptor drum and the transfer roller to transfer images on the photoreceptor drum to a paper fed by them. In order to obtain higher quality of images on the paper, the paper velocity at the roller transfer unit should be kept constant.

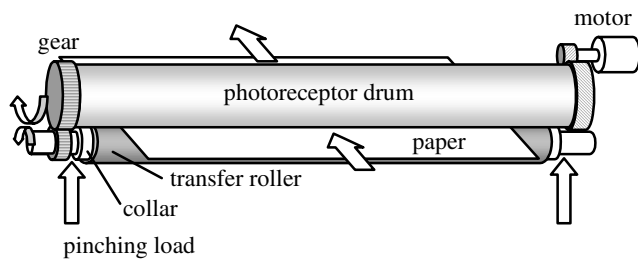


Figure 1. The schematic view of the roller transfer unit.

The paper velocity at the roller transfer unit, which is affected by several factors, is difficult to estimate and to control directly. First, the paper velocity is different from the roller one because of a slip between them. Furthermore, the difference between the photoreceptor drum and the transfer roller is generally applied for higher transfer efficiencies. Secondly, as shown in Figure 2, the pushing or pulling tension from the registration rollers and the fuser rollers modulates the paper velocity at the roller transfer unit.^{1,2}

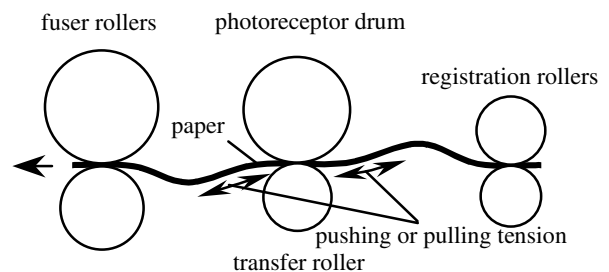


Figure 2. The schematic diagram of the paper feeding around the roller transfer unit.

Accordingly, the paper velocity prediction requires the slip characteristics of the rollers, the tensions in the paper and a physical model that binds the above essentials.

Objectives

The objectives are to develop a numerical method predicting the paper velocity at the roller transfer unit in an electrophotographic system and to verify the prediction by comparing the numerical results with experiments.

Scheme of Prediction of Paper Velocity

The proposed scheme predicting a paper velocity is composed of the expression of forces in the paper at each unit and the construction of the equilibrium equations of the forces. The forces in the paper at the roller transfer unit, as

shown in Figure 3, consist of two tractions that exerted by slips from the photoreceptor drum and the transfer roller and two tensions from the registration rollers and the fuser rollers. As shown in Figure 3, all the arrows for the force and the velocity in the following figures are set up to be toward the direction of the paper feeding and are defined as the positive direction.

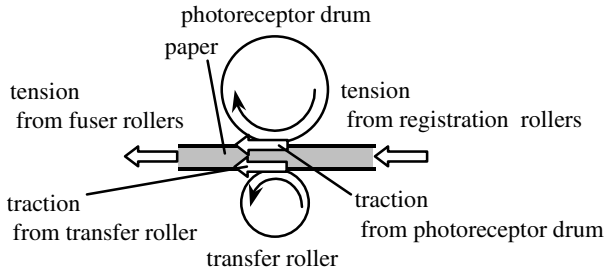


Figure 3. The schematic diagram of forces in the paper at the roller transfer unit.

1. Expression of Traction

The traction is modeled considering slip characteristics that are derived from the measurement³ shown in Figure 4 of the relative velocity between the driving roller and a paper under an external force. A slip ratio $S_{driving\ roller}$ is defined as follows,

$$S_{driving\ roller} = (V_{driving\ roller} - V_{paper}) / V_{driving\ roller} \quad (1)$$

where $V_{driving\ roller}$ and V_{paper} are the roller and the paper velocities, respectively. The slip ratio is changed by the external force, which corresponds with the traction due to the paper in equilibrium of forces. Because the traction is also a friction force between the driving roller and the paper, the traction is proportional to a pinching load as follows,

$$Tr = F = (F/P) \times P, \quad (2)$$

where Tr is the traction, F is the external force and P is the pinching load. F/P in eq.(2) is generally defined as a traction efficiency, which is characterized by the slip ratio shown in Figure 5. Accordingly, the traction is further expressed by the traction efficiency $\mu_{t,driving\ roller}$ as follows,

$$Tr = \mu_{t,driving\ roller} \times P. \quad (3)$$

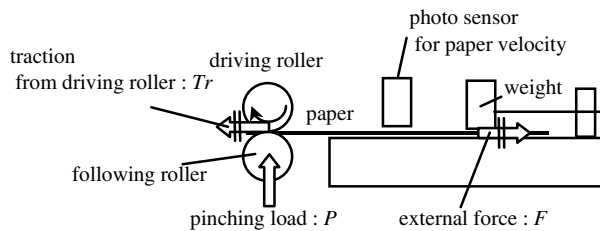


Figure 4. The schematic diagram of measuring instrument of slip ratios.

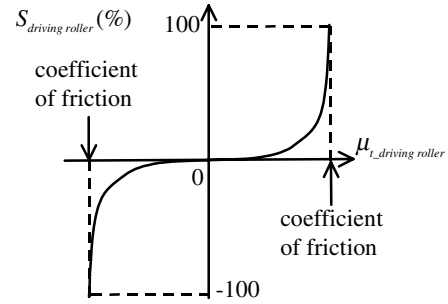


Figure 5. The general slip characteristics.

2. Model of Tension

The tension in the paper between the units is calculated using the paper feeding simulation⁴. As shown in Figure 6, the tensions in the paper between the first rollers and the second those are specified by the change of the paper length between the units, which is as follows,

$$\Delta L_{first\ rollers\ to\ second\ rollers} = \sum \delta t \times (V_{first\ rollers} - V_{second\ rollers}), \quad (4)$$

where $\Delta L_{first\ rollers\ to\ second\ rollers}$, $V_{first\ rollers}$, $V_{second\ rollers}$ and δt are the change of the paper length between the units, the velocities of the first and the second rollers and a paper feeding time step, respectively. $\Delta L_{first\ rollers\ to\ second\ rollers}$ is equal to zero before the paper reaches the second rollers.

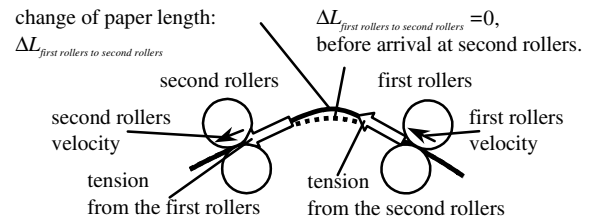


Figure 6. The schematic diagram of tensions in the paper between units.

3. Equilibrium Equation of Forces

The equilibrium equation of the forces in the paper at each unit is constructed using the expression of the traction and the tension. The equation of the paper velocity is also formulated by the definition of the slip. The total equations in all the units, which are based on the valuables in Figure 7 and 8, are as follows,

At the registration rollers :

$$T_{regist+} + \mu_{t,regist} \times P_{regist} = 0. \quad (5)$$

$$V_{P,regist} = V_{R,regist} (1 - S_{regist}). \quad (6)$$

At the roller transfer unit :

$$T_{transfer+} + (\mu_{t,photo} + \mu_{t,transfer}) \times P_{transfer} + T_{transfer-} = 0. \quad (7)$$

$$V_{P,transfer} = V_{R,photo} (1 - S_{photo}). \quad (8)$$

$$V_{P_transfer} = V_{R_transfer} (1 - S_{transfer}). \quad (9)$$

At the fuser rollers :

$$T_{fuser-} + \mu_{t_fuser} \times P_{fuser} = 0. \quad (10)$$

$$V_{P_fuser} = V_{R_fuser} (1 - S_{fuser-}), \quad (11)$$

where the following symbols are used in the above equations.

$T_{regist+}$: tension from the roller transfer unit at the registration rollers, which is the function of the change of the paper length between the registration rollers and the roller transfer unit

P_{regist} : pinching load at the registration rollers

V_{P_regist} : paper velocity at the registration rollers

μ_{t_regist} : traction efficiency between the registration roller and a paper

S_{regist} : slip ratio between the registration roller and a paper, which is the function of μ_{t_regist}

V_{R_regist} : registration roller velocity

$T_{transfer-}$: tension from the registration rollers at the roller transfer unit, which is the function of the change of the paper length between the registration rollers and the roller transfer unit

$T_{transfer+}$: tension from the fuser rollers at the roller transfer unit, which is the function of the change of the paper length between the roller transfer unit and the fuser rollers

$P_{transfer}$: pinching load at the roller transfer unit

$V_{P_transfer}$: paper velocity at the roller transfer unit

μ_{t_photo} : traction efficiency between the photoreceptor drum and a paper

$\mu_{t_transfer}$: traction efficiency between the transfer roller and a paper

S_{photo} : slip ratio between the photoreceptor drum and a paper, which is the function of μ_{t_photo}

$S_{transfer}$: slip ratio between the transfer roller and a paper, which is the function of μ_{t_regist}

V_{R_photo} : photoreceptor drum velocity

$V_{R_transfer}$: transfer roller velocity

T_{fuser-} : tension from the roller transfer unit at the fuser rollers, which is the function of the change of the paper length between the roller transfer unit and the fuser rollers

P_{fuser} : pinching load at the fuser rollers

V_{P_fuser} : paper velocity at the fuser rollers

μ_{t_fuser} : traction efficiency between the fuser roller and a paper

S_{fuser} : slip ratio between the fuser roller and a paper, which is the function of μ_{t_fuser}

V_{R_fuser} : fuser roller velocity

The slip at the fuser rollers is difficult to characterize due to the fuser and the toner and is assumed to be zero in the following section. Then, the paper velocity at the fuser rollers is set up to be equal to the fuser rollers velocity.

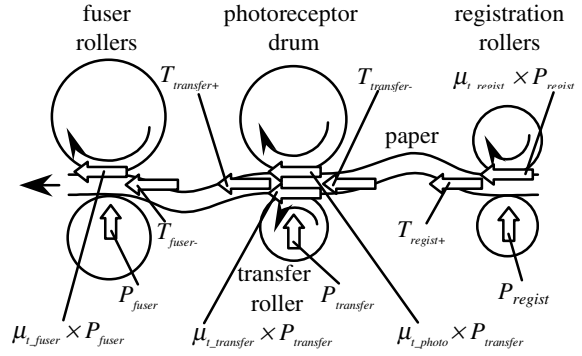


Figure 7. The schematic diagram of forces in the paper.

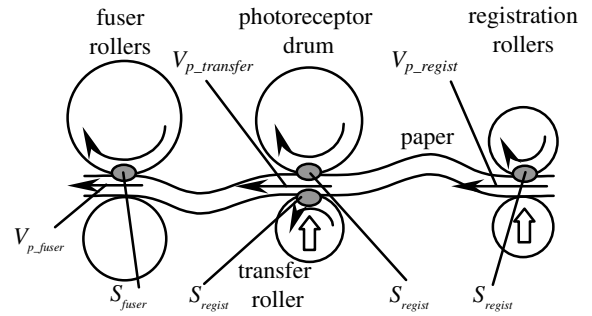


Figure 8. The schematic diagram of slip ratios.

4. Algorithm of Calculation

In order to sequentially calculate the paper velocity at the roller transfer unit, $T_{regist+}$, V_{P_regist} , μ_{t_regist} , S_{regist} , $T_{transfer-}$, $V_{P_transfer}$, μ_{t_photo} , $\mu_{t_transfer}$, S_{photo} , and $S_{transfer}$, are added the super script n to as the valuables at the n-th paper feeding step and are solved by the valuables at n-1-th one. Then, $T_{regist+}^n$, $T_{transfer-}^n$ and $T_{transfer+}^n$ are implicitly described by the change of the paper length at the n-1-th paper feeding step and the paper velocity at the n-th one as follows,

$$\left. \begin{aligned} T_{regist+}^n &= TF_{regist+} (\Delta L_{regist\ to\ transfer}^{n-1} \\ &\quad + \delta t \times (V_{P_regist}^n - V_{P_transfer}^n)), \text{ (before passing by} \\ &\quad \text{the registration rollers)} \\ &= 0. \text{ (after passing by the registration rollers)} \end{aligned} \right\} \quad (12)$$

$$\left. \begin{aligned} T_{transfer-}^n &= TF_{transfer-} (\Delta L_{regist\ to\ transfer}^{n-1} \\ &\quad + \delta t \times (V_{P_regist}^n - V_{P_transfer}^n)), \text{ (before the paper} \\ &\quad \text{passing by the registration rollers)} \\ &= 0. \text{ (after passing by the registration rollers)} \end{aligned} \right\} \quad (13)$$

$$\left. \begin{aligned} T_{transfer+}^n &= 0, \text{ (before arrival at the fuser rollers)} \\ &= TF_{transfer+} (\Delta L_{transfer\ to\ fuser}^{n-1}) \end{aligned} \right\}$$

$$+ \delta t \times (V_{P_transfer}^n - V_{P_fuser}^n), \quad (14)$$

(after arrival at the fuser rollers)

$$\Delta L_{regist\ to\ transfer}^n = \Delta L_{regist\ to\ transfer}^{n-1} + \delta t \times (V_{P_regist}^n - V_{P_transfer}^n), \quad (15)$$

$$\Delta L_{transfer\ to\ fuser}^n = \Delta L_{transfer\ to\ fuser}^{n-1} + \delta t \times (V_{P_transfer}^n - V_{P_fuser}^n), \quad (16)$$

where $TF_{regist+}$, $TF_{transfer-}$ and $TF_{transfer+}$ are the tension functions, which are the subsets of $T_{regist+}$, $T_{transfer-}$ and $T_{transfer+}$, respectively. Each function is specified by the change of the paper length between the units to be obtained using the paper feeding simulation. $\Delta L_{regist\ to\ transfer}^{n-1}$, $\Delta L_{regist\ to\ transfer}^n$, $\Delta L_{transfer\ to\ fuser}^{n-1}$ and $\Delta L_{transfer\ to\ fuser}^n$ are the changes of the paper length at each step, respectively. V_{P_fuser} is the paper velocity at the fuser rollers and is assumed to agree with the fuser rollers velocity.

Experimental Results for Forces

1. Results for Traction

In order to model the tractions at the registration rollers, the photoreceptor drum and the transfer roller shown in Table 1, the slip ratios are measured using the instrument shown in Figure 4 and are shown in Figure 9. The slip ratio versus the negative traction efficiency that is not shown in Figure 9 is assumed to be symmetric with respect to the point that a traction efficiency equals zero.

Table 1. The Driving Roller Characteristics.

The registration roller	Diameter (mm) : 15.2 Stiffness (JISA) : 80
The photoreceptor drum	Diameter (mm) : 30.0
The transfer roller	Diameter (mm) : 16.2 Stiffness (ASKERC) : 42
The fuser roller	Diameter (mm) : 30.9

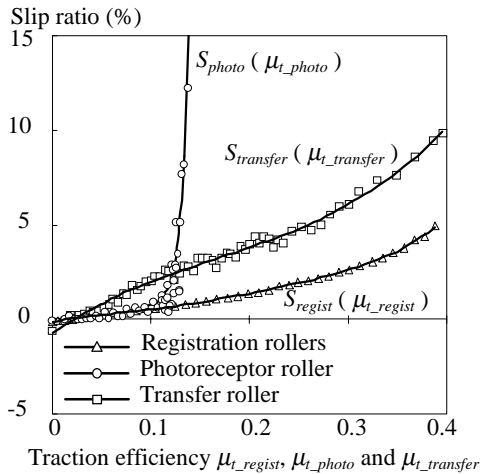
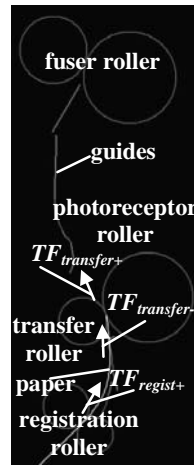
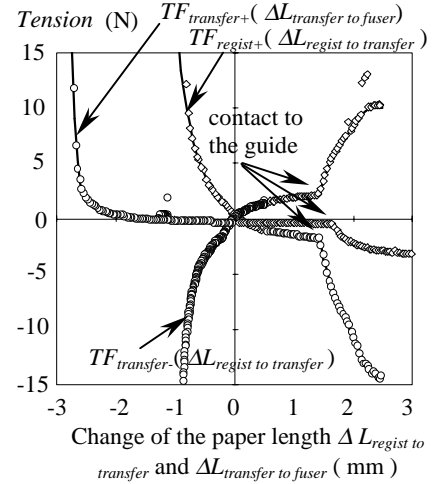


Figure 9. Measured slip characteristics.



(a)



(b)

Figure 10. (a)The paper feeding layout around the roller transfer unit and (b) the calculated tension.

2. Results for Tension

We prepared the experimental apparatus for the prediction and the verification of our model, which is composed of the models of the registration rollers, the roller transfer unit and the fuser rollers. The A3-sized paper feeding is calculated in the layout shown in Figure 10-(a) to obtain the tensions shown in Figure 10-(b). The tension functions $TF_{regist+}$, $TF_{transfer-}$ and $TF_{transfer+}$ specified in Figure 10-(b) correspond to the tensions shown in Figure 10-(a). Each tension varies with the change of the paper length between the units. The elbow-shaped bends shown in Figure 10-(b) are abrupt changes of the tension with a paper contacting to the guide.

Prediction and Experimental Results

The paper velocities at the roller transfer unit in two cases of the transfer roller velocities are calculated under the condition of the roller velocity in Table 2 and the layout shown in Figure 10-(a).

Table 2. The Roller Velocities.

The registration rollers (mm/s)	114.2	
The photoreceptor drum (mm/s)	110.3	
The transfer roller (mm/s)	118.5	114.7
The fuser rollers (mm/s)	113.8	

In case that the transfer roller velocity is 118.5 (mm/s), the paper velocity predicted at the roller transfer unit is plotted in Figure 11. The points <A>, and <C> in Figure 11 correspond to the snapshots shown in Figure 12. The paper velocity gradually decreases until the paper arrives at the fuser rollers due to the pull of the paper from the registration rollers, and is almost constant until the paper passes by the registration rollers. When the paper passes by the registration rollers, the paper velocity abruptly

ly increases because the tension from the registration rollers at the roller transfer unit is removed. Until the paper passes by the roller transfer unit, the paper velocity gradually decreases due to the push of the paper from the fuser rollers. The experimental result is also plotted in Figure 11, which is measured by the time interval sensing of the pattern of lines printed on papers. The simulation throughout the paper feeding at the roller transfer unit approximates the average of the experiment, which shows a fluctuation with the rotational frequency of the registration rollers.

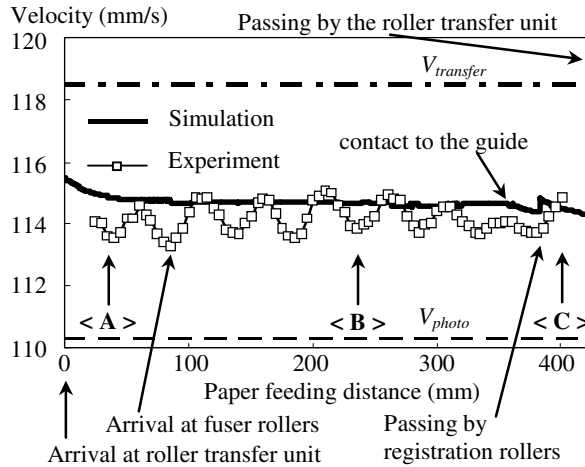


Figure 11. The paper velocities at the roller transfer in case that the transfer roller velocity equals 118.5mm/s.

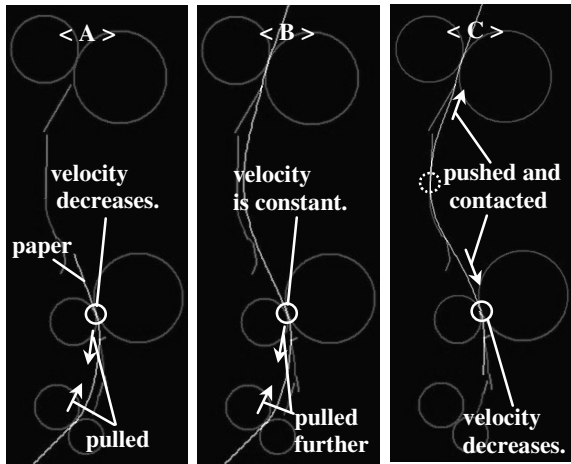


Figure 12. The simulated shapes of the paper in case that the transfer roller velocity equals 118.5mm/s.

The other case that the velocity of the transfer roller is 114.7(mm/s) is shown in Figure 13 and 14. The points <a>, and <c> in Figure 13 also correspond to the snapshots shown in Figure 14. First, the prediction gives the increase due to the push of the paper from the registration rollers. Then, the prediction increases further at the contact to the guide. Since then, the prediction is constant until the paper

passes by the registration rollers. When the paper passes by the registration rollers, the prediction suddenly decreases. As the final stage, the prediction gradually increases due to the pull of the paper from the fuser rollers. The above changes of the paper velocity predicted during the paper feeding at the roller transfer unit agree well with those of the experimental result.

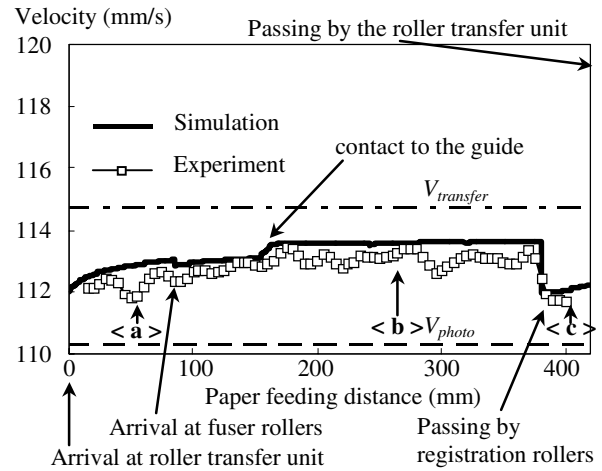


Figure 13. The paper velocities at the roller transfer unit in case that the transfer roller velocity equals 114.7mm/s.

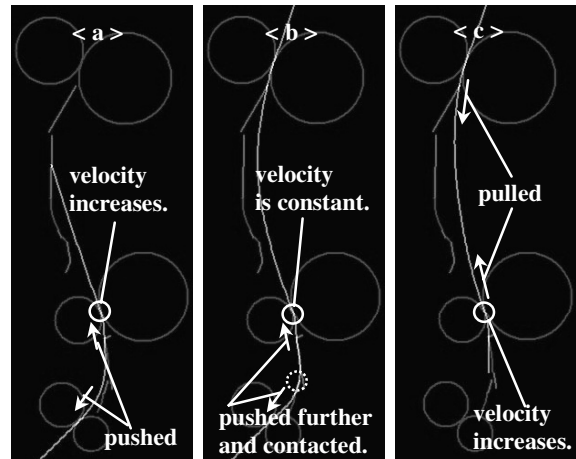


Figure 14. The simulated shapes of the paper in case that the transfer roller velocity equals 114.7mm/s.

Conclusion

We propose a new method that predicts the paper velocity at the roller transfer unit considering the roller slip characteristics and the tension in the paper. The predicted velocities show the excellent agreement with those from experiments. Our method captures well the change of the paper velocity during the paper feeding.

References

1. Osamu Takehira and Yuko Hayama, *Japan Hardcopy 2001 Fall Meeting*, pg. 60. (2001)
2. Osamu Takehira and Yuko Hayama, *ICIS'02, Tokyo*, pg. 674. (2002)
3. Masanobu Segawa and Nobuaki Omata, *OMRON TECHNICS*, **37**, pg. 151. (1997)
4. Osamu Takehira, *11th Symposium on ISPS*, (2000)

Biography

Satoshi Okano received his B.S. degree in physics from University of Chuo, Japan in 1991. He joined Ricoh in 1991 as a member of research scientist, and has been working in the area of computational dynamics. Recently he has been working on the field of electrophotography.